ELSEVIER

Journal of Alloys and Compounds 452 (2008) 67–72

Journal of ALLOYS AND COMPOUNDS

www.elsevier.com/locate/jallcom

Determination of phase equilibria in the Fe_3Al–Cr–Mo–C semi-quaternary system using a new diffusion-multiple technique

Satoru Kobayashi *, Stefan Zaefferer

Department of Microstructure Physics and Metal Forming, Max Planck Institute für Eisenforschung GmbH, Max-Planck-Str. 1, D-40237 Düsseldorf, Germany

Received 18 September 2006; received in revised form 21 December 2006; accepted 15 January 2007
Available online 22 February 2007

Abstract

A new diffusion-multiple (DM) technique was proposed to allow us mapping of quaternary phase diagrams. This technique utilizes a combination of DM technique to introduce two-dimensional composition gradients in a matrix phase and a conventional annealing heat treatment to have precipitation reactions in the matrix. Phase equilibria at 800 °C in the semi-quaternary Fe_3Al–Cr–Mo–C system were determined with an assist from this technique. The following five carbide phases were precipitated in the Fe_3Al matrix phase (B2) with composition gradients of Cr, Mo and C: κ-Fe_3AlC, M_6C_H, M_6C_L, Cr_7C_3 and M_2C (M: Mo, Cr and Fe, the two M_6C phases are distinguished by their C and Cr contents.). It was found from our DM technique that the four-phase equilibrium of $M_6C_H + M_6C_L + Cr_7C_3 + B2$ exists. Microstructure analysis of several bulk alloys as well as DM samples revealed that the three-phase equilibrium of $M_6C_L + \kappa + B2$ in the Fe_3Al–Mo–C system changes to that of $M_6C_L + Cr_7C_3 + B2$ with increasing Cr content through the following three four-phase equilibria: (1) $M_6C_H + M_6C_L + \kappa + B2$, (2) $M_6C_H + Cr_7C_3 + \kappa + B2$, (3) $M_6C_H + M_6C_L + Cr_7C_3 + B2$. The M_2C phase is thought to be not in equilibrium with the Fe_3Al matrix phase at 800 °C.

Keywords: Intermetallics; Precipitation; Diffusion; Microstructure; Phase diagrams

1. Introduction

The use of diffusion-multiples is a powerful technique to map ternary phase diagrams, as proposed by Zhao and coworkers [1,2]. A diffusion-multiple is a dense assembly of three or more different metal pieces. The multiple is subjected to high temperature to allow interdiffusion reactions along two-dimensional composition gradients. The interdiffusion among the elements forms all the intermetallic compounds and solid-solution phases in that ternary system. Advanced microanalyses to characterize phases make diffusion-multiples a high efficiency approach for mapping phase diagrams. Zhao made a comparison of several ternary systems obtained from both diffusion-multiple technique and the conventionally equilibrated alloy method, and showed the reliability and efficiency of the diffusion-multiple technique [2].

On the other hand, the conventionally equilibrated alloy method determines phase equilibria in bulk materials using phase transformations, especially precipitation reactions that occur by decrease in temperature due to the reduction of solubility of a solute element. The disadvantage of this method is that extremely large experimental efforts are required to determine phase diagrams in multi-component systems.

Recently we are proposing a new technique that allows us mapping of quaternary phase diagrams by a combination of two-dimensional composition gradients introduced by the diffusion-multiple technique and precipitation reactions caused by annealing heat treatment, which will be explained in detail in Section 2.1. In this paper phase equilibria in the semi-quaternary Fe_3Al–Cr–Mo–C system were determined with an assist from this technique.

2. Experimental technique

2.1. Principles of quaternary phase diagram mapping using our diffusion-multiple technique

A combination of diffusion-multiple technique to introduce two-dimensional composition gradients and annealing to have precipitation reactions is utilized

* Corresponding author. Present address: Osaka Center for Industrial Materials Research, Institute for Materials Science, Tohoku University, 1-1 Gakuen-cho Naka-ku, Sakai Osaka 599-8531, Japan. Tel.: +81 72 252 1161x5654; fax: +81 72 254 9912.
E-mail address: kobayashi@imr.tohoku.ac.jp (S. Kobayashi).

0925-8388/$ – see front matter © 2007 Elsevier B.V. All rights reserved.
doi:10.1016/j.jallcom.2007.01.171

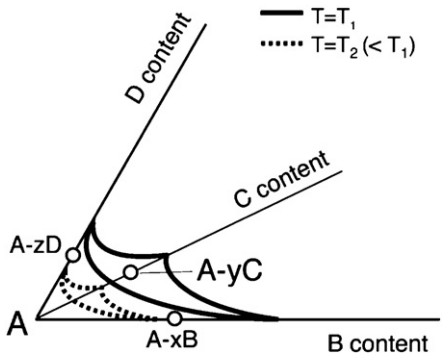

Fig. 1. Schematic A-rich part quaternary phase diagram showing how to obtain all the precipitate phases that are in equilibrium with the A rich α phase in the system.

to obtain phase equilibria between a matrix phase, α, and all the precipitate phases that are in equilibrium with the α phase: three kinds of binary alloys (**A-xB**, **A-yC**, **A-zD**) are selected in such way that additional elements B, C and D, respectively, are soluble in the A-rich α phase at a high temperature, T_1, as shown in Fig. 1. These alloys are joint and heat-treated at T_1, to introduce two-dimensional composition gradients among the elements A to D in the α matrix phase. A subsequent heat treatment at a lower temperature (annealing), T_2, reduces the solubility of each element, which allows precipitation of all phases that are in equilibrium with the matrix phase (α) in that quaternary system. By analysis of phases present around the sample interfaces and the triple point after prolonged annealing time, it should be possible to map out tie-lines between α phase and precipitate phases.

2.2. Experimental procedures

The following three kinds of ternary alloys were chosen as end members to determine phase equilibria in the Fe_3Al–Cr–Mo–C system based on literature reported on the ternary phase diagrams [3–5]: (1) Fe–26Al–5Cr, (2) Fe–27Al–10Mo, (3) Fe–27Al–2C (at.%). Hereafter the alloys are designated by 5Cr, 10Mo and 2C, respectively. The matrix phase, B2, (Structurbericht notation is used through this paper) with approximate composition of Fe–(27–28)Al is regarded as one component. These alloys were prepared from 3N purity iron, 4N aluminium, 3N chromium, 3N molybdenum and 3N carbon by induction melting in an argon atmosphere.

Since the diffusions of Mo and Cr are much slower than that of carbon, the two pieces of 10Mo and 5Cr were first coupled. Pieces of 5 mm × 10 mm × 30 mm were cut from the ingot, coupled as schematically shown in Fig. 2 and clamped between two austenitic stainless steel plates using ferritic stainless steel screws. The surfaces for welding were ground, mechanically polished and electropolished with ethanol containing 8% perchloric acid under the conditions of 28 V, 10–15 °C for 20 s. This sample was heat-treated at 800 °C for 24 h for welding and at 1200 °C for 24 h for creating a long-range diffusion zone of Mo and Cr. Heat treatments were performed in a SiO_2 tube in argon gas back filled after evacuation to 6×10^{-4} Pa. This diffusion-couple was cut into pieces of 10 mm × 10 mm × 5 mm and then coupled with the piece of 2C (see Fig. 2), and heat-treated at 800 °C for 24 h and at 1200 °C for 15 min followed by water quenching. This sample was cut into halves (see Fig. 2) and the cross-section of the one piece was used for microstructure analysis. The other piece was annealed at 800 °C for 300 h in the argon atmosphere.

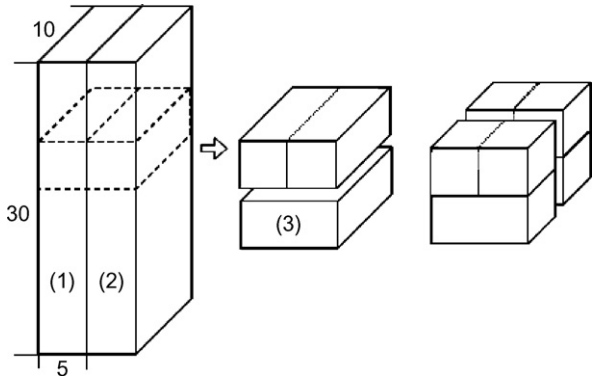

Fig. 2. Procedures to fabricate a diffusion-multiple sample.

Microstructure was examined by optical microscopy (OM) and high resolution scanning electron microscopy (HRSEM) with a backscattered electron (BSE) detector, energy dispersive spectrometry (EDS) and electron backscatter diffraction (EBSD) camera. Phases present were identified by a combination of EDS and EBSD. For the EDS analyses, calibration curves were made to correlate the intensities of Fe, Al, Cr and Mo with their compositions by using several as-cast alloys as standards with the assumption that the nominal compositions and the alloy compositions are equal. The carbon contents in carbide phases were determined by subtracting the compositions of the substitutional elements from 1: $x_C = 1 - (x_{Fe} + x_{Al} + x_{Cr} + x_{Mo})$. Experimentally obtained EBSD patterns were fitted with simulated patterns of a certain types of phases which we can expect based on compositional data by EDS. Simulated patterns were obtained by calculating structure factors for electron diffraction from the known atom positions in phases using the EDAX/TSL software Delphi and the computer program TOCA [6,7]. Some examples of EBSD patterns fitted by the simulation are shown in Fig. 3.

3. Results and discussion

3.1. Microstructure of the diffusion-multiple after heat treatment at 1200 °C

Fig. 4 shows the cross-section of our diffusion-multiple sample after heat treatment to introduce two-dimensional composition gradients of Cr, Mo and C in the B2 matrix. This sample was successfully coupled and long range composition gradients were created, as seen by microstructure and chemical analyses along the lines (a) and (b) (see also Fig. 5). Along the horizontal direction in the 10Mo and 5Cr parts, Mo and Cr diffused about 1000 and 2000 μm, respectively (Fig. 5(a)). Along the vertical direction, the Mo and Cr concentration gradients are also visible in the composition profiles (Fig. 5(b)) even though the diffusion time was short. The carbon concentration gradient can be recognized by the type and the volume fraction of carbide phases. In the 2C part κ-Fe_3AlC ($E2_1$) carbide phase existed homogeneously in the matrix before coupled, but it can be seen that the volume fraction of the phase decreases with approaching the 10Mo/5Cr part after coupled (Fig. 4). The κ phase is also visible in the 5Cr part in the vicinity of the original interface with the 2C part, which clearly demonstrates that carbon concentration gradient exists across the interface. The coarse and needle shape precipitate observed in the 10Mo part was identified as M_6C ($E9_3$) carbide phase. The morphology and the large size of the phase indicate that this phase was grown from the 10Mo/2C interface during heat treatment at 1200 °C. Very fine M_2C ($B8_1$) carbide phase was found between the coarse M_6C carbides although this carbide is not visible in the OM picture.

3.2. Microstructure of the diffusion-multiple after annealing at 800 °C

Fig. 6 shows optical microstructure taken in the vicinity of the triple junction of the original interfaces in the diffusion-multiple

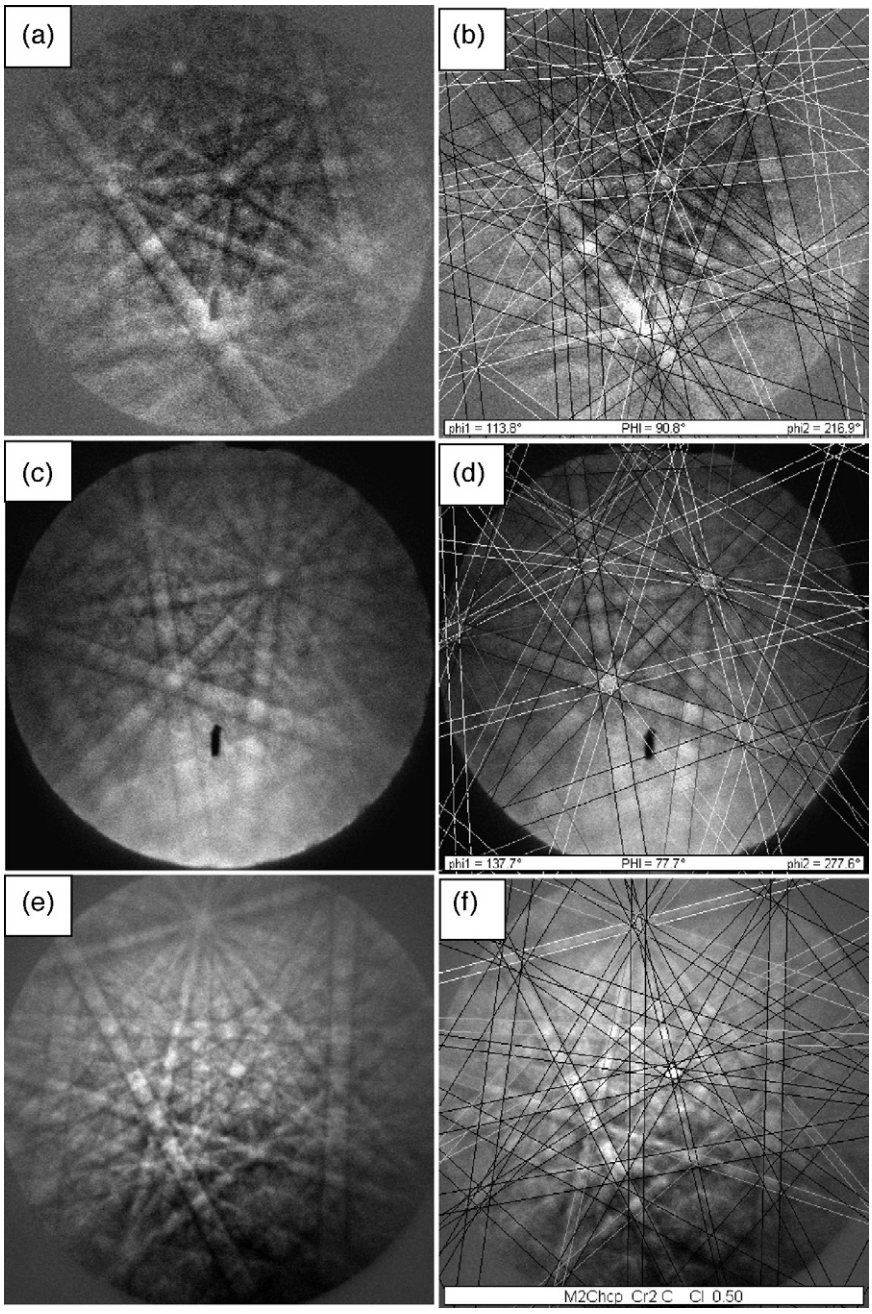

Fig. 3. Experimentally obtained EBSD patterns (a, c, and e) and the patterns fitted with simulated patterns (b, d, and f) for: (a and b) Cr_7C_3 ($D10_1$), (c and d) M_6C ($E9_3$), and (e and f) M_2C ($B8_1$).

sample annealed at 800 °C for 300 h. Four types of carbide structures were observed in the B2 matrix: κ-Fe_3AlC ($E2_1$), M_6C ($E9_3$), M_2C ($B8_1$) and Cr_7C_3 ($D10_1$). The areas on which the carbide phases are found are also shown in this figure. In the 5Cr part, Cr_7C_3 carbide was precipitated in the vicinity of the 5Cr/2C interface but κ carbide disappears after annealing. When moving into the direction to 10Mo part, M_6C and M_2C phases appear in this order.

Two distinguished compositions were detected in the M_6C carbide phase by EDS analysis although their crystal structures were not distinguished by our EBSD analyses. Table 1 exhibits their compositions, the one designated by M_6C_H, contains higher C and Cr content than the other, designated by M_6C_L. These coarse M_6C phases are well in contact with Cr_7C_3 phase, as seen in Fig. 7(a). This microstructure reminds us that in this DM technique it is possible to make similar microstructure analysis to that in the conventional bulk alloy method to discuss phase equilibria. We can assume from the microstructure of Fig. 7(a) that the four-phase coexisting region of $M_6C_H + M_6C_L + Cr_7C_3 + B2$ exists in this system. Microstructures obtained from other areas such as 2–5 in Fig. 6 give us interesting information that the Cr_7C_3 carbide phase is in equilibrium with the M_6C_L phase in the Cr-rich matrix compositions, while in equilibrium with the M_6C_H phase in the Cr-poor

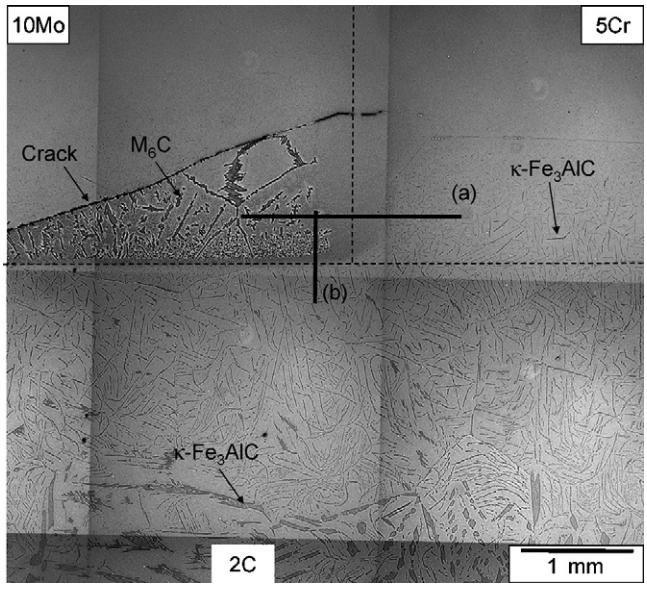

Fig. 4. Optical microstructure showing the cross-section of the diffusion-multiple sample heat-treated at 1200 °C. The original interfaces are drawn by broken lines in this figure.

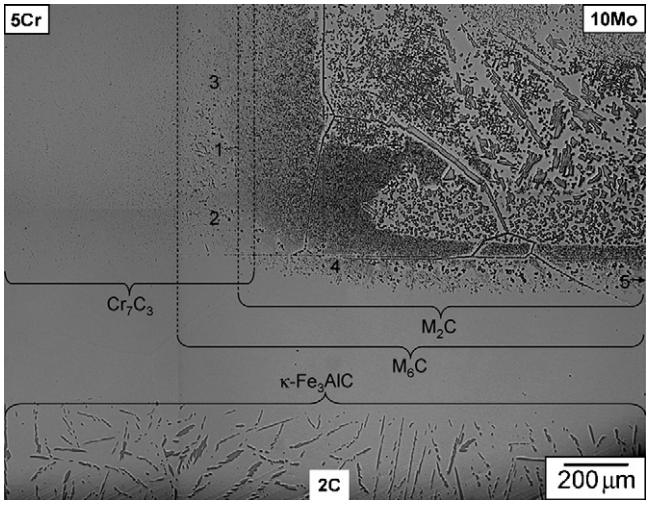

Fig. 6. Optical microstructure showing the vicinity of the triple junction in the diffusion-multiple sample annealed at 800 °C for 300 h. It is noted that the position of the 5Cr part and the 10Mo part in this sample is opposite to that in the sample in Fig. 4.

composition range. This observation can be explained using Fig. 8(a) in which the four-phase region of $M_6C_H + M_6C_L + Cr_7C_3 + B2$ is drawn in the isothermal tetrahedron with the apices of (Fe–28Al), Cr, Mo and C. The composition of M_6C_L phase exists on the Cr-rich side of the tetrahedron. It is, therefore, reasonable that the Cr-poor M_6C_L phase is formed on the Cr-rich side of the four-phase region and the Cr-rich M_6C_H on the Cr-poor side.

The M_2C carbide phase is, on the other hand, rarely in contact with the other carbide phases. In grain boundaries the fine distribution of this carbide is not observed and the coarse M_6C_H phase replaces it (Fig. 7(b)). These observations suggest that the M_2C phase is metastable and not in equilibrium with the B2 matrix phase. We also found that tie-lines between the compositions

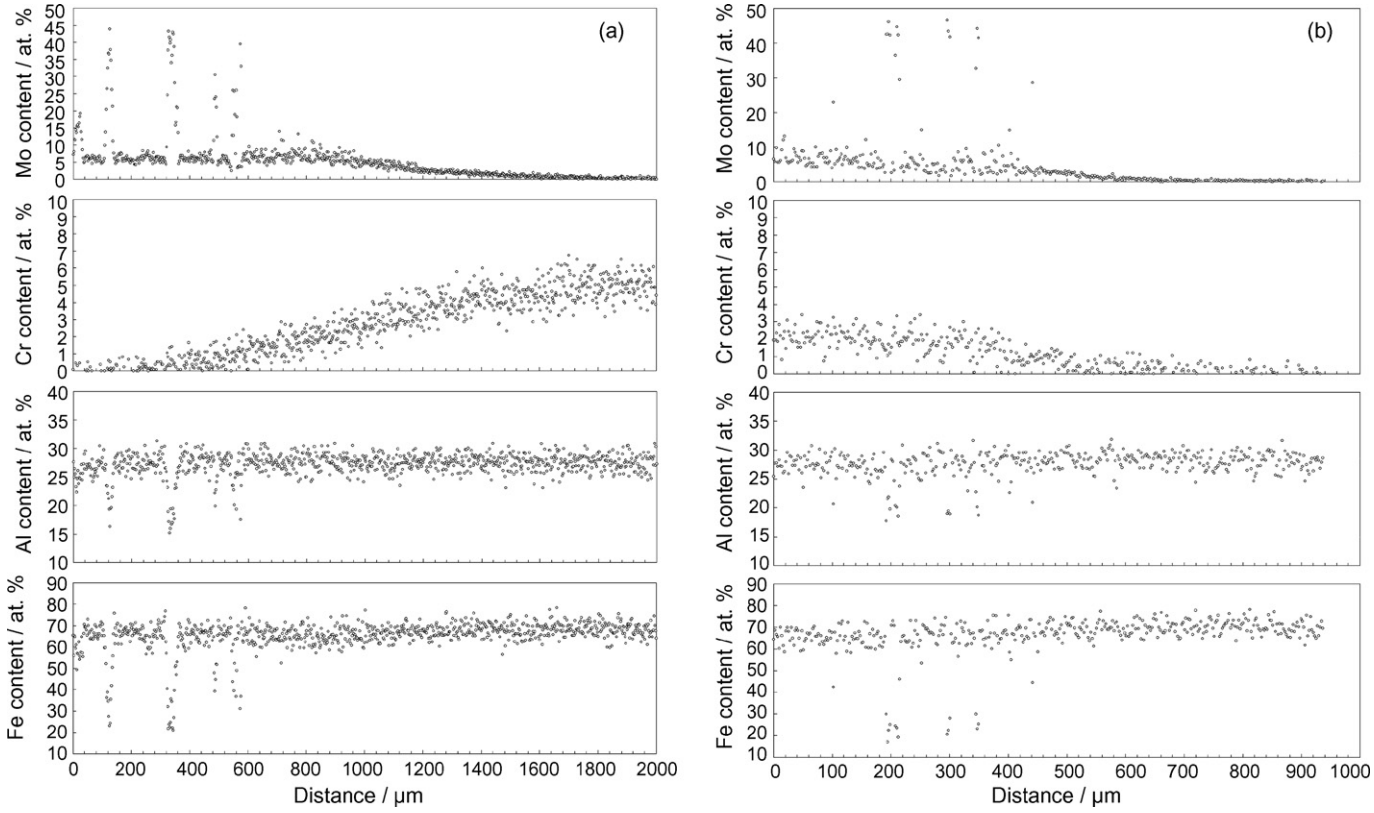

Fig. 5. Concentration profiles of Mo, Cr, Al and Fe taken from the lines (a) and (b) in Fig. 4.

Table 1
Phases and their compositions obtained from the areas marked in Fig. 6 in the diffusion-multiple sample annealed at 800 °C for 300 h

Area analysed	Phase present	Phase composition				
		Fe	Al	Cr	Mo	C
1	M_6C_H	14.5	13.6	9.7	45.0	17.2
	M_6C_L	22.1	16.4	3.3	45.0	13.2
	Cr_7C_3	16.3	1.0	50.5	2.2	30.0
	Matrix	68.6	27.9	2.6	0.9	–
2	M_6C_H	14.4	14.2	9.8	44.2	17.4
	Cr_7C_3	19.3	0.9	47.1	2.8	29.9
	Matrix	68.7	28.1	2.4	0.8	–
3	M_6C_L	22.3	16.0	3.5	43.9	14.3
	Cr_7C_3	14.1	1.0	52.1	2.7	30.1
	Matrix	69.0	27.2	2.9	0.9	–
4	M_6C_H	16.4	12.4	5.2	47.2	18.8
	M_6C_L	22.3	16.0	1.6	46.0	13.8
	Matrix	70.4	27.8	1.0	0.8	–
5	M_6C_L	22.8	15.9	0	47.2	14.1
	Matrix	71.2	28.0	0	0.8	–

The EDS analysis is not precise enough to detect the carbon concentration in the matrix phase.

obtained from M_2C particles and the matrix go through the four-phase tetrahedron of $M_6C_H + M_6C_L + Cr_7C_3 + B2$. This result supports the thought that M_2C is not thermodynamically stable within the B2 matrix at this temperature. In the 10Mo part far away from the original interfaces with 5Cr and 2C parts, μ-$(Fe,Al)_7Mo_6$ ($D8_5$) phase and Mo_3Al (A15) phase were precipitated, which is a reasonable result according to literature [3].

Another thing which should be noted here is that the κ carbide disappears in the matrix containing Cr and Mo. The reason of the disappearing of κ phase is not yet understood, but we assume that it is because the carbon in the κ phase may be attracted by more stable Cr_7C_3 and M_6C carbide phases and this reaction is faster than the Cr and Mo diffusion toward the 2C part. Nevertheless, this result makes it impossible to determine phase relationship between κ phase and the other carbide phases in the composition range of high C/M (M: Cr, Mo) ratios, as recognized in Fig. 8(a).

3.3. Isothermal tetrahedron of the Fe_3Al–Cr–Mo–C system

Several bulk alloys were made to cover the composition range of the high C/M ratios and their microstructures were determined

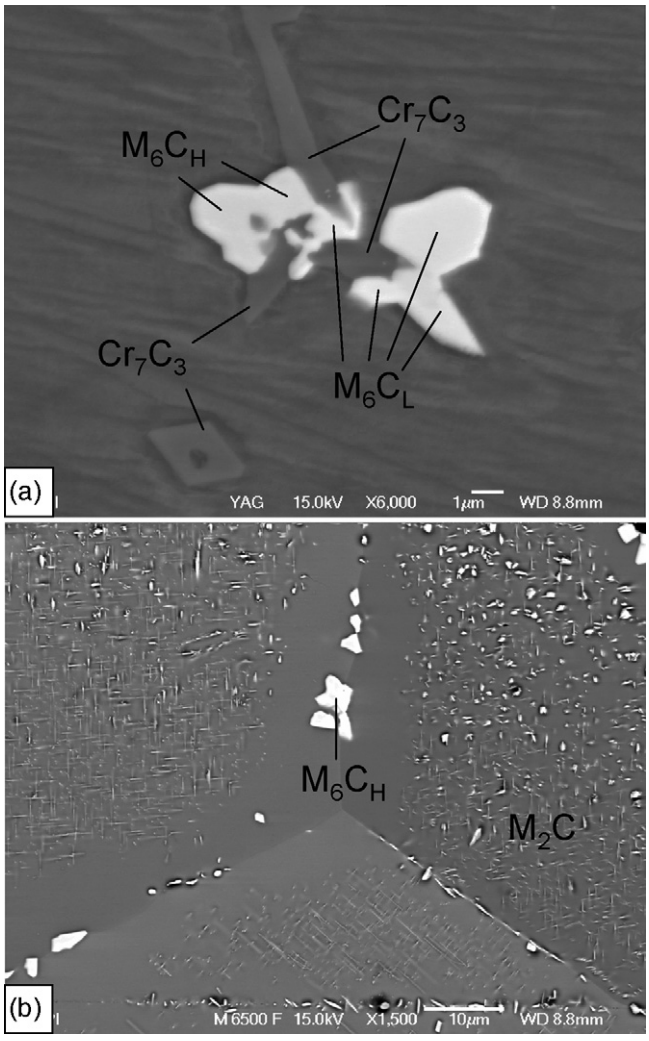

Fig. 7. Backscattered electron images taken from the diffusion-multiple sample shown in Fig. 6: (a) from the area 1. Lines observed in the matrix are scratches from polishing, (b) close to the triple junction.

in the conventional method. The equilibrium phases in those alloys after heat treatment at 800 °C for 1000 h are summarized in Table 2. It is found from the first alloy containing 2Cr that κ phase is in equilibrium with M_6C_H, Cr_7C_3 and the B2 matrix phase. The compositions of M_6C_H, Cr_7C_3 phases measured in this alloy are found to be similar to those of the phases obtained in the area 1 and 2 in the diffusion-multiple sample. On the

Table 2
The equilibrium phases and their compositions obtained from some bulk Fe_3Al-based alloys annealed at 800 °C for 1000 h

Bulk alloy composition					Phase present	Phase composition				
Fe	Al	Cr	Mo	C		Fe	Al	Cr	Mo	C
Balance	25.9	2.0	1.0	1.2	M_6C_H	15.5	13.5	8.4	44.0	18.6
					Cr_7C_3	22.4	0.7	45.0	2.8	29.1
					κ-Fe_3AlC	61.0	22.4	3.8	0.2	12.6
					Matrix	70.2	27.7	1.5	0.6	–
Balance	26.4	0	1.0	1.2	M_6C_L	23.2	15.2	0	47.0	14.6
					κ-Fe_3AlC	65.5	22.6	0	0.2	11.7
					Matrix	71.8	27.6	0	0.6	–

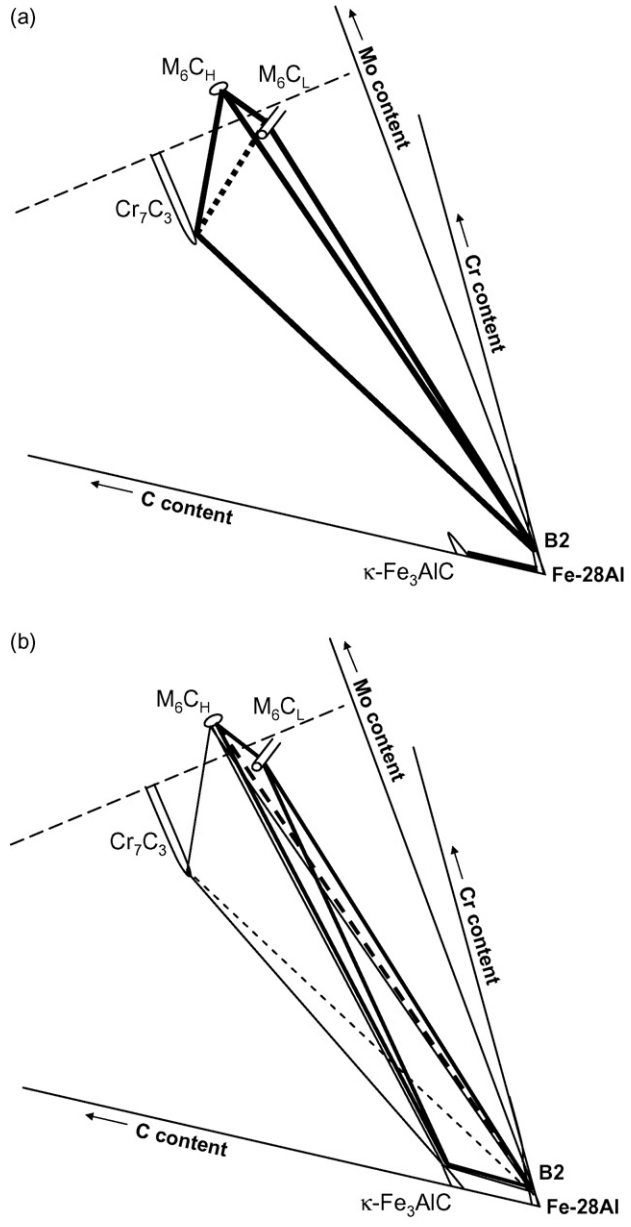

Fig. 8. Isothermal tetrahedron in the Fe_3Al-rich corner of the Fe_3Al–Cr–Mo–C semi-quaternary system showing: (a) the four-phase coexisting region of $M_6C_H + M_6C_L + Cr_7C_3 + B2$ in the Cr-rich composition range and (b) the four-phase coexisting regions of $M_6C_H + Cr_7C_3 + \kappa + B2$ (thinner lines) and $M_6C_H + M_6C_L + \kappa + B2$ phases (thicker lines) in the Cr-poor composition range.

other hand, κ phase is in equilibrium with M_6C_L and B2 matrix phase in the second sample containing no Cr. It is noted that the composition of the M_6C_L phase is in good agreement with that of the same phase observed in the diffusion-multiple sample (compare area 5 in Tables 1 and 2) to tell how accurate our diffusion-multiple technique is.

Based on the results obtained from our DM technique and the conventional bulk alloy method, phase equilibria at 800 °C in the (Fe_3Al)–Cr–Mo–C system are discussed. In the Fe_3Al–Mo–C system the three-phase coexisting region of $\kappa + M_6C_L + B2$ exists. However, the Cr addition makes the M_6C_H and Cr_7C_3 carbide phases thermodynamically stable. Taking the phase rules into account, it is reasonable to conclude that phase equilibrium changes from the three-phase equilibrium of $M_6C_L + \kappa + B2$ to that of $M_6C_L + Cr_7C_3 + B2$ through the following three four-phase equilibria with increasing Cr content:

$$M_6C_H + M_6C_L + \kappa + B2 \text{ (see thicker lines in Fig.8(b))} \quad (1)$$

$$M_6C_H + Cr_7C_3 + \kappa + B2 \text{ (see thinner lines in Fig.8(b))} \quad (2)$$

$$M_6C_H + M_6C_L + Cr_7C_3 + B2 \text{ (see Fig.8(a))} \quad (3)$$

4. Conclusion

A new diffusion-multiple (DM) technique to allow us mapping of quaternary phase diagrams was proposed. This technique utilizes a combination of two-dimensional composition gradients in a matrix phase introduced by DM technique and precipitation reactions in the matrix by annealing. Phase equilibria at 800 °C in the semi-quaternary Fe_3Al–Cr–Mo–C system were determined with an assist from this technique. The results obtained are as follows:

(1) The following five carbide phases were detected in the Fe_3Al matrix phase (B2) with composition gradients of Cr, Mo and C: κ-Fe_3AlC, M_6C_H, M_6C_L, Cr_7C_3 and M_2C (M: Mo, Cr and Fe, and the two M_6C phases are distinguished by their C and Cr contents).
(2) It was found from our DM technique that the four-phase equilibrium of $M_6C_H + M_6C_L + Cr_7C_3 + B2$ exists in the composition range of low C/M ratios. It was, however, not successful to obtain phase equilibria in the composition range with high C/M ratios.
(3) Based on the microstructure analysis of our DM samples and several bulk alloys, it is concluded that phase equilibrium changes from the three-phase equilibrium of $M_6C_L + \kappa + B2$ to that of $M_6C_L + Cr_7C_3 + B2$ through the following three four-phase equilibria as Cr content increases: (1) $M_6C_H + M_6C_L + \kappa + B2$, (2) $M_6C_H + Cr_7C_3 + \kappa + B2$, and (3) $M_6C_H + M_6C_L + Cr_7C_3 + B2$.
(4) The M_2C phase is not in equilibrium with the Fe_3Al matrix phase at 800 °C.

Acknowledgements

The authors would like to thank Mr. Kraus Markmann, Mr. Gerhard Bialkowski, Jürgen Baseler and Ralf Selbach of the Max-Planck-Institute for Iron Research for their help with the experiments.

References

[1] J.C. Zhao, J. Mater. Sci. 39 (2004) 3913–3925.
[2] J.C. Zhao, M.R. Jackson, L.A. Peluso, Acta Mater. 51 (2003) 6395–6405.
[3] M. Eumann, M. Palm, G. Sauthoff, Steel Res. Int. 75 (2004) 62–73.
[4] M. Palm, G. Inden, Intermetallics 3 (1995) 443–454.
[5] G. Petzow, G. Effenberg, Ternary Alloys 8, VCH Verlagsgesellschaft, Stuttgart, 1993, pp. 324–343.
[6] S. Zaefferer, Adv. Imag. Electron Phys. 125 (2002) 355–415.
[7] S. Zaefferer, JEOL News 39 (2004) 10.